

# The $^{15}\text{O}(\alpha, \gamma)^{19}\text{Ne}$ Breakout Reaction and Impact on X-Ray Bursts

W. P. Tan,\* J. L. Fisker, J. Görres, M. Couder, and M. Wiescher  
*Department of Physics, University of Notre Dame, Notre Dame 46556*

The breakout reaction  $^{15}\text{O}(\alpha, \gamma)^{19}\text{Ne}$ , which regulates the flow between the hot CNO cycle and the rp-process, is critical for the explanation of the burst amplitude and periodicity of X-ray bursters. We report on the first successful measurement of the critical  $\alpha$ -decay branching ratios of relevant states in  $^{19}\text{Ne}$  populated via  $^{19}\text{F}({}^3\text{He}, t)^{19}\text{Ne}$ . Based on the experimental results and our previous lifetime measurements of these states, we derive the first experimental rate of  $^{15}\text{O}(\alpha, \gamma)^{19}\text{Ne}$ . The impact of our experimental results on the burst pattern and periodicity for a range of accretion rates is analyzed.

An X-ray burster is characterized by a repeated sudden increase of X-ray emission within only a few seconds to a total energy of about  $10^{39-40}$  ergs [1]. The recurrence time between single bursts can range from hours to days. The characteristics of X-ray burst phenomena are being studied extensively today using a number of space-based X-ray observatories such as RXTE, BeppoSAX, Chandra, HETE-2, and XMM/Newton. More than eighty galactic sources of X-ray bursts have been identified since their initial discovery in 1976 [2]. These bursts are explained as thermonuclear explosions in the atmosphere of an accreting neutron star in a close binary system [3, 4]. When critical values for density and temperature are reached in the neutron star atmosphere, the freshly accreted hydrogen and helium ignites and burns via the hot,  $\beta$ -limited CNO cycles at a constant rate [5]. Depending on the strength of the  $^{15}\text{O}(\alpha, \gamma)^{19}\text{Ne}$  reaction, break-out from the hot CNO cycles will occur, fueling the rapid proton capture (rp)-process [6, 7]. The rp-process converts the light element fuel into heavy elements from Fe-Ni up to Cd-Sn within only a few seconds.

The strength of the  $^{15}\text{O}(\alpha, \gamma)^{19}\text{Ne}$  break-out reaction not only regulates the ignition point of the actual burst but affects also the burst recurrence rate. However, the large experimental uncertainties of the  $^{15}\text{O}(\alpha, \gamma)^{19}\text{Ne}$  reaction rate prevented the use of the rate as a tool to identify the conditions required for the ignition and the recurrence time of the bursts. Quite the opposite, a comparison between astronomical observations and theoretical model predictions was used to constrain the reaction rate [8, 9]. Fisker et al. demonstrated that the previous speculative estimate on the lower limit of the reaction rate would lead to burst quenching for observed accreting rates of  $\dot{M} \sim 10^{17} \text{g s}^{-1}$  [9]. This suggested that the previous lower limit estimate was too low. Cooper et al. on the other hand performed an analytical stability study suggesting that the widely used rate of Langanke et al. [10] might be too high [8]. An experimental study of  $^{15}\text{O}(\alpha, \gamma)^{19}\text{Ne}$  is clearly necessary. It will not only reduce the wide range of uncertainty on the actual ignition conditions but may also provide new constraints on accretion itself by identifying the transition point between the thermonuclear runaway in the burst [11] and steady state burning as expected for higher accretion rates [12].

There have been many attempts in the past to provide

experimental data for determining the  $^{15}\text{O}(\alpha, \gamma)^{19}\text{Ne}$  reaction rate. While progress has been made, the presently used rates are still relying mainly on theoretical estimates [5, 10]. The  $^{15}\text{O}(\alpha, \gamma)^{19}\text{Ne}$  reaction rate is expected to be dominated by a single resonance level at an excitation energy of 4.03 MeV in  $^{19}\text{Ne}$  [10] where the resonant rate is defined by  $N_A \langle \sigma v \rangle_{res} \propto (kT)^{-3/2} (2J + 1) \Gamma_\gamma \Gamma_\alpha / \Gamma \exp(-E/kT)$ . Present intensities of radioactive  $^{15}\text{O}$  beams are insufficient for a direct measurement. Therefore, past studies have focused mainly on the use of indirect techniques by measuring the characteristic nuclear structure features of the  $^{19}\text{Ne}$  compound nucleus for the determination of the resonance parameters for the reaction rate [13, 14, 15, 16, 17, 18, 19, 20]. Yet none of the studies were successful in determining a model independent reaction rate with well defined experimental limits.

Recently excitation energies and  $\gamma$  partial widths  $\Gamma_\gamma$  or the inverse of lifetimes of the states in  $^{19}\text{Ne}$  near  $\alpha$ -threshold have been measured with the improved Doppler shift attenuation method [20]. The result on the lifetime of the 4.03-MeV state was also confirmed in an independent measurement at TRIUMF [21]. The remaining quantity to be determined is the  $\alpha$ -decay branching ratios  $B_\alpha = \Gamma_\alpha / \Gamma$  that have mostly been estimated from the  $\alpha$  strengths of the mirror states in  $^{19}\text{F}$  with large systematic model dependent uncertainties inherent to the DWBA analysis of  $\alpha$ -transfer reactions on  $^{15}\text{N}$  [10, 14, 22]. Several attempts have been made in the past to measure the relative  $\alpha$ -decay widths directly [13, 17, 18, 23]. While this approach was successful for higher-lying states in  $^{19}\text{Ne}$ , it failed for the critical levels near the  $\alpha$  threshold due to the low decay branching.

Here we report, for the first time, the successful laboratory measurement of  $\alpha$  decay of the unbound states in  $^{19}\text{Ne}$  which provides an experimental rate for  $^{15}\text{O}(\alpha, \gamma)^{19}\text{Ne}$  and discuss the astrophysical implications.

The  $^{19}\text{F}({}^3\text{He}, t)$  reaction was used to populate  $\alpha$  unbound states in  $^{19}\text{Ne}$ ; their  $\alpha$ -decay branchings were determined through  $t$ - $\alpha$  coincidence measurements. The detection system was optimized for the measurement of low energy  $\alpha$  particles ( $\leq 1$  MeV) and an overall detection efficiency sufficient for probing branching ratios as low as  $10^{-4}$ .

A schematic drawing of the experimental setup is shown in Fig. 1. The  ${}^3\text{He}$  beam of 24 MeV was produced at the FN tandem accelerator of the University of Notre Dame

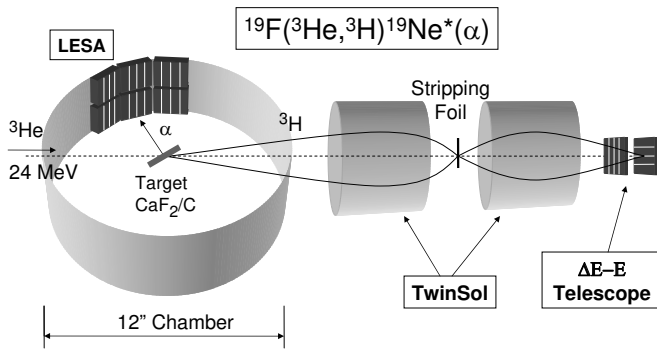


FIG. 1: Schematic setup of this experiment is shown (not to scale for better presentation).

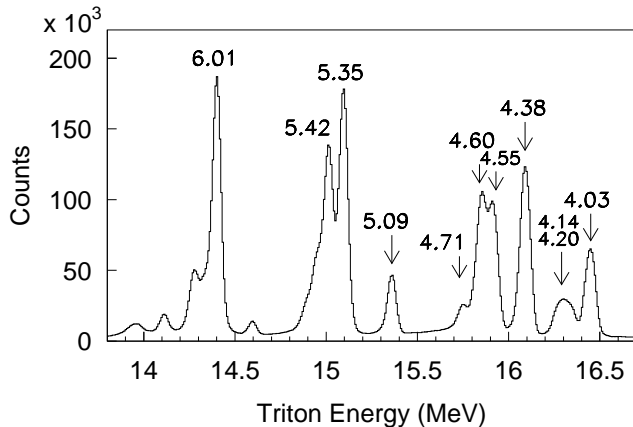


FIG. 2: The total energy spectrum of tritons detected in the telescope is shown using the  $\Delta E$ - $E$  particle identification technique. Peaks related to the excited states in  $^{19}\text{Ne}$  are labelled.

to bombard a  $40 \mu\text{m}/\text{cm}^2$  thick  $\text{CaF}_2$  target evaporated on a  $20 \mu\text{m}/\text{cm}^2$  thick Carbon foil. The TwinSol facility at Notre Dame, a dual in-line superconducting solenoid ion-optical system [24], was used as a large-acceptance momentum separator to separate tritons from other reaction products. The acceptance range corresponded to a solid angle of 50 msr. A large area position-sensitive  $\Delta E$ - $E$  telescope consisting of two  $500 \mu\text{m}$  thick silicon detectors was positioned close to the focal plane of TwinSol to identify and track tritons.

A Low Energy Silicon-strip Array (LESA) was designed to detect the low energy  $\alpha$  particles from the decay of the excited states in  $^{19}\text{Ne}$ . The array consists of six identical  $300 \mu\text{m}$  thick silicon-pad detectors, each of which has 4 strips and an area of  $4 \times 4 \text{ cm}^2$ . To reduce the detection threshold the dead layer was limited to a thickness of  $< 0.05 \mu\text{m}$ . This translates into an energy loss of  $< 14 \text{ keV}$  for  $200 \text{ keV}$   $\alpha$  particles. The particle identification in LESA was achieved by measuring the particle's energy and time of flight from the target to LESA.

In Fig. 2, the triton energy spectrum is presented and demonstrates the good separation that was achieved for the

excited states in  $^{19}\text{Ne}$ . In particular, the 4.03-MeV state is well separated although the two high spin states at 4.14 and 4.20 MeV are not resolved. Furthermore, enough counts were collected to ensure that the sensitivity of the measurements of  $\alpha$  decay branching ratios reaches as low as  $10^{-4}$ . However, double hits in the telescope inevitably contribute to the background in the triton spectrum in Fig. 2. In rare cases, double-hit events with high energy electrons can contaminate a given triton peak with tritons from higher-lying states ( $> 0.5 \text{ MeV}$  higher in energy). The effect on small  $\alpha$  decay branching fractions is demonstrated below.

A detailed discussion and analysis of the experimental results will be presented in a forthcoming paper [25]. Here we only summarize our results and focus on the aspects relevant for the determination of the reaction rate. Kinetically corrected  $\alpha$  spectra for the decay of the observed  $^{19}\text{Ne}$  states are shown in Fig. 3 after appropriate triton and timing gates are applied. The total and background  $\alpha$  spectra are presented in the left panels while the net spectra are plotted in the right panels. The background was obtained from random coincidence events outside of the  $\alpha$  timing gates which have a much larger count rate than those within the gates for rare  $\alpha$  decay cases. For this reason, the additional statistical error from the determination of the background does not contribute significantly to the uncertainty of the net spectra. The background rise to the low energy end is due to the energy loss of high energy electrons in LESA. The coincident  $\alpha$ s from the corresponding states are indicated by the shaded areas while the structures at higher energy are  $\alpha$ s leaking from higher-lying states with much larger  $B_{\alpha}$ s because of double hit events with high energy electrons. Fortunately, the double-hitting electrons deposit at least 0.5 MeV in the telescope and the resulting 0.5 MeV gap is sufficient to separate these  $\alpha$ s from the weak  $\alpha$  decay signals for the states at 4.03-4.38 MeV.

While the  $\alpha$  group for the decay of the 4.55-MeV state in  $^{19}\text{Ne}$  is quite pronounced – similar to the decay of the higher excited states at 4.60, 4.71, and 5.09 MeV – only weak  $\alpha$ -decay branching ratios on the order of  $10^{-3}$  or less are observed for the levels near the  $\alpha$  threshold.

The present experiment yields for the first time branching ratios for the states at 4.03-4.38 MeV near the alpha threshold. An  $\alpha$ -decay branching ratio of  $2.9 \pm 2.1 \times 10^{-4}$  was measured for the 4.03-MeV state consistent with previous upper limits of  $< 4.3 \times 10^{-4}$  [17] and  $< 6 \times 10^{-4}$  [18]. The two states at 4.14 and 4.20 MeV could not be resolved, but a combined branching ratio of  $1.2 \pm 0.5 \times 10^{-3}$  was determined. This is surprisingly large compared to previous predictions and assessments [10, 18]. The measured  $\alpha$  peak seems to be lower in energy than the simulated one indicating that these decay events are more likely from the 4.14-MeV state. As for the 4.38-MeV state, the present result of  $1.2 \pm 0.3 \times 10^{-3}$  agrees with the stringent upper limit of  $< 3.9 \times 10^{-3}$  [17] while it differs from previously given values of  $0.044 \pm 0.032$  [13] and  $16 \pm 5 \times 10^{-3}$  [18] which were handicapped by poor statistics and lack of experimen-

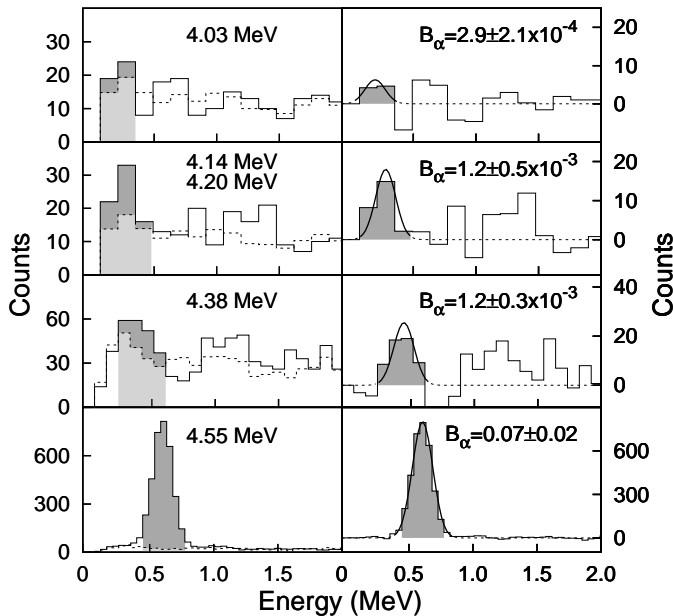


FIG. 3: Kinematically corrected  $\alpha$  energy spectra are shown in coincidence with the tritons for the lower lying states at 4.03-4.55 MeV. Left panels: the solid histograms indicate all coincidence events while the dashed histograms show the background normalized from large ensemble of random coincidence events; the shaded areas present the expected  $\alpha$  energy range for the corresponding states in  $^{19}\text{Ne}$ . Right panels: the net  $\alpha$  spectra are shown after the background deduction; the smooth curves are simulated calculations assuming a decay branching as measured. See text for details.

tal resolutions. For the states at higher excitation energies of 4.55-5.09 MeV our new measurements show excellent agreement with the previous results [13, 16, 17, 18, 19].

The reaction rate for  $^{15}\text{O}(\alpha,\gamma)^{19}\text{Ne}$  was directly calculated from the measured  $\alpha$ -decay branching ratios and the lifetimes [20] of the  $\alpha$ -unbound states in  $^{19}\text{Ne}$ . Fig. 4 shows the reaction rate as a function of temperature. The upper and lower limits of the rate are based on the experimental uncertainties of the branching ratio and lifetime measurements. Also shown for comparison is the range of previous theoretical uncertainty [9].

The new experimental rate allows not only a better identification of the ignition conditions of X-ray bursts but permits also the improved analysis of the dynamics and mechanism of X-ray bursts. In this context the accretion rate corresponding to the transition point between steady state and unstable burning is of particular interest.

The impact of the  $^{15}\text{O}(\alpha,\gamma)^{19}\text{Ne}$  rate has been investigated in the framework of a dynamical and self-consistent spherically symmetric X-ray burst model [9]. This model couples a modified version of a general relativistic hydrodynamics code [26] with a generic nuclear reaction network [27] using the operator-split method. By solving the general relativistic equations, the nuclear reaction flow, the conductive, radiative, and convective heat transport was

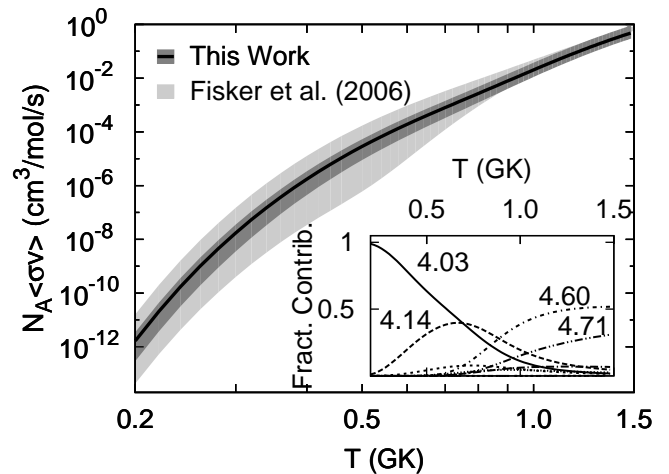


FIG. 4: The new  $^{15}\text{O}(\alpha,\gamma)^{19}\text{Ne}$  reaction rate (black line) is plotted with one sigma uncertainty indicated by the dark-grey area. The uncertainty range discussed by Fisker et al. [9] are indicated by the light-grey area which did not take into account the uncertainty from high-lying ( $> 4.4$  MeV) states that contribute significantly at  $T > 0.6$  GK. The inset displays the fractional contributions of the individual resonance states to the reaction rate.

computed in a spherically symmetric geometry. More detailed discussions of the model can be found in a forthcoming paper by Fisker et al [28].

The transition between unstable burning and steady state burning is easily observable by the change in burst pattern. The associated accretion rate, however, correlates only on average with the observed accretion luminosity [29]. The influence of the nuclear trigger processes on the actual transition point can therefore only be investigated in the framework of a theoretical calculation.

Previous simulations [11, 30] and calculations [31] have determined the transition point to be around  $\dot{M} \sim 2.1 \times 10^{18} \text{g s}^{-1}$  for a fiducial neutron star with  $R = 10$  km and  $M = 1.4M_{\odot}$  adopting a solar composition for the accreted matter. However, the importance of the uncertainty of the  $^{15}\text{O}(\alpha,\gamma)^{19}\text{Ne}$  reaction was not taken into account. With the new measurement, we are now able to determine the transition point between steady state burning and unstable burning with significantly improved accuracy. We performed several calculations for different accretion rates while tracking the luminosity resulting from the nuclear burning. The results shown in Fig. 5 depict how the burning becomes stable for  $\dot{M} \geq 1.9 \times 10^{18} \text{g s}^{-1}$ .

We performed identical calculations for the one sigma upper and lower limits as shown in Fig. 4. The upper limit yields the same transition accretion rate, whereas the lower limit increases the transition point to  $\dot{M} \approx 2.1 \times 10^{18} \text{g s}^{-1}$ . The uncertainty in the determination of the accretion rate at transition point is thus about 10% compared to previous uncertainties of one order of magnitude [9]. Further model studies of the transition accretion rate are necessary to take

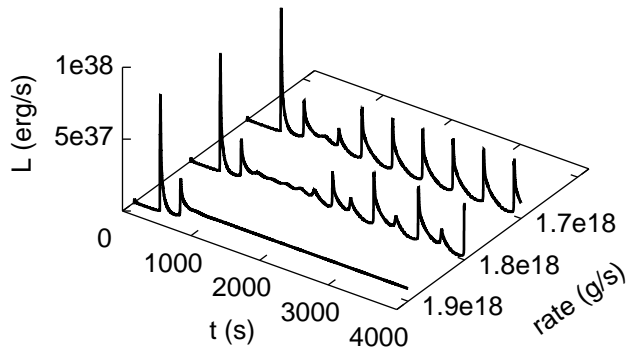


FIG. 5: We used the newly measured rate to calculate the luminosity originating from the nuclear burning as a function of time for different accretion rates. As is seen from the constant luminosity on the graph, the burning is stable for  $\dot{M} \geq 1.9 \times 10^{18} \text{ g s}^{-1}$ .

better into account the mass and radius of the neutron star as well as the accreted composition.

This work shows the importance of laboratory results for providing stringent limits for the burning conditions in stellar objects. It demonstrates how experimental nuclear data can complement observational results and provide important insights for the astrophysical model simulations. The  $^{15}\text{O}(\alpha, \gamma)^{19}\text{Ne}$  reaction is the key for our understanding of the onset of X-ray bursts. The experimental results bring us closer to a better understanding of the complex interplay between fuel supply and burning processes at the extreme conditions of the neutron star atmosphere.

We thank M. Beard, A. Couture, S. Falahat, L. Lamm, P. J. LeBlanc, H. Y. Lee, S. O'Brien, A. Palumbo, E. Stech and E. Strandberg for help during the course of the experiment. This work is supported by the National Science Foundation under grant No. PHY01-40324 and the Joint Institute for Nuclear Astrophysics ([www.jinaweb.org](http://www.jinaweb.org)), NSF-PFC under grant No. PHY02-16783.

---

\* Electronic address: [wtan@nd.edu](mailto:wtan@nd.edu)

[1] S. E. Woosley, et al., *Astrophys. J. Suppl.* **151**, 75 (2004).

- [2] D. K. Galloway, et al., *astro-ph/0608259*.
- [3] S. E. Woosley and R. E. Taam, *Nature* **263**, 101 (1976).
- [4] P. C. Joss, *Nature* **270**, 310 (1977).
- [5] M. Wiescher, J. Görres, and H. Schatz, *J. Phys. G* **25**, R133 (1999).
- [6] H. Schatz, et al., *Phys. Rep.* **294**, 167 (1998).
- [7] R. K. Wallace and S. E. Woosley, *Astrophys. J. Suppl.* **45**, 389 (1981).
- [8] R. L. Cooper and R. Narayan, *Astrophys. J. Lett.* **648**, L123 (2006).
- [9] J. L. Fisker, J. Görres, M. Wiescher, and B. Davids, *Astrophys. J.* **650**, 332 (2006).
- [10] K. Langanke, M. Wiescher, W. A. Fowler, and J. Görres, *Astrophys. J.* **301**, 629 (1986).
- [11] J. L. Fisker, W. R. Hix, M. Liebendörfer, and F.-K. Thielemann, *Nucl. Phys. A* **718**, 614 (2003).
- [12] H. Schatz, L. Bildsten, A. Cumming, and M. Wiescher, *Astrophys. J.* **524**, 1014 (1999).
- [13] P. V. Magnus, et al., *Nucl. Phys. A* **506**, 332 (1990).
- [14] Z. Q. Mao, H. T. Fortune, and A. G. Lacaze, *Phys. Rev. Lett.* **74**, 3760 (1995).
- [15] G. Hackman, et al., *Phys. Rev. C* **61**, 052801(R) (2000).
- [16] A. M. Laird, et al., *Phys. Rev. C* **66**, 048801 (2002).
- [17] B. Davids, et al., *Phys. Rev. C* **67**, 065808 (2003).
- [18] K. E. Rehm, et al., *Phys. Rev. C* **67**, 065809 (2003).
- [19] D. W. Visser, et al., *Phys. Rev. C* **69**, 048801 (2004).
- [20] W. P. Tan, et al., *Phys. Rev. C* **72**, 041302(R) (2005).
- [21] R. Kanungo, et al., *Phys. Rev. C* **74**, 045803 (2006).
- [22] F. de Oliveira, et al., *Nucl. Phys. A* **597**, 231 (1996).
- [23] M. Kurokawa, et al., in *International Symposium on Origin of Matter and Evolution of Galaxies 97*, edited by S. Kubono, T. Kajino, K. I. Nomoto, and I. Tanihata (World Scientific, Singapore; New Jersey, 1998), p. 245.
- [24] F. Becchetti, et al., *Nucl. Instr. Meth. Phys. Res. A* **505**, 377 (2003).
- [25] W. P. Tan, et al., in preparation.
- [26] M. Liebendörfer, S. Rosswog, and F.-K. Thielemann, *Astrophys. J. Suppl.* **141**, 229 (2002).
- [27] W. R. Hix and F.-K. Thielemann, *J. Comput. Appl. Math.* **109**, 321 (1999).
- [28] J. L. Fisker, et al., to be published in *Astrophys. J.*
- [29] W. H. G. Lewin, et al., *Astrophys. J.* **319**, 893 (1987).
- [30] A. Heger, A. Cumming, and S. E. Woosley, *astro-ph/0511292*.
- [31] I. Fushiki and D. Q. Lamb, *Astrophys. J.* **323**, L55 (1987).